

# Characterization of the Emergence of Order in an Oscillated Granular Layer

Daniel I. Goldman,<sup>1</sup> Gemunu H. Gunaratne,<sup>2,3</sup> M. D. Shattuck,<sup>1</sup> Donald J. Kouri,<sup>2,4</sup> David K. Hoffman,<sup>5</sup> D. S. Zhang,<sup>4</sup> and Harry L. Swinney<sup>1</sup>

<sup>1</sup> Center for Nonlinear Dynamics, The University of Texas at Austin, Austin, TX 78712

<sup>2</sup> The Department of Physics, University of Houston, Houston, TX 77204

<sup>3</sup> The Institute of Fundamental Studies, Kandy, Sri Lanka

<sup>4</sup> The Department of Chemistry, University of Houston, Houston, TX 77204

<sup>5</sup> Department of Chemistry and Ames Laboratory, Iowa State University, Ames, IO 50011

The formation of textured patterns has been predicted to occur in two stages. The first is an early time, domain-forming stage with dynamics characterized by a disorder function  $\bar{\delta}(\beta) \sim t^{-\sigma_E}$ , with  $\sigma_E = \frac{1}{2}\beta$ ; this decay is universal. Coarsening of domains occurs in the second stage, in which  $\bar{\delta}(\beta) \sim t^{-\sigma_L}$ , where  $\sigma_L$  is a nonlinear function of  $\beta$  whose form is system and model dependent. Our experiments on a vertically oscillated granular layer are in accord with theory, yielding  $\sigma_E \approx 0.5\beta$ , and  $\sigma_L$  a nonlinear function of  $\beta$ .

PACS number(s): 05.70.Ln, 82.40.Ck, 47.54.+r

The formation of textured spatial patterns has been studied in laboratory experiments [1] and model systems [2]. Several quantities have been used to describe the development of patterns represented by a scalar field  $v(\mathbf{x})$  with a typical wavevector  $k_0$ , including the structure factor [4–7], density of topological defects [8], and a recently introduced family of characterizations called the disorder function,

$$\bar{\delta}(\beta) = \frac{(2 - \beta) \int d^2x |(\Delta + k_0^2)v(\mathbf{x})|^\beta}{\int d^2x \frac{k_0^{2\beta} \langle |v(\mathbf{x})| \rangle^\beta}{k_0^{2\beta} \langle |v(\mathbf{x})| \rangle^\beta}}, \quad (1)$$

where  $\langle |v(\mathbf{x})| \rangle$  denotes the mean of  $|v(\mathbf{x})|$ , and  $\bar{\delta}(\beta)$  ( $0 \leq \beta < 2$ ) has been normalized to be scale invariant [9].  $\bar{\delta}(\beta)$  describes configuration-independent aspects of textures and their formation, aspects that are independent under repetition of the experiment. It can be used to study multiple aspects of patterns just as generalized dimensions [10] and singularity spectra [11] can be used to describe multiple aspects of strange attractors. In experiments presented in this paper, we characterize the time evolution of patterns in a vertically oscillated granular layer using  $\bar{\delta}(\beta)$ .

Before describing our experiments, we review numerical and analytical work on the coarsening of patterns after a quench from an initial featureless (or noisy) state. Most studies have focused on solutions  $u(\mathbf{r}, t)$  to the Swift-Hohenberg equation [2],

$$\frac{\partial u}{\partial t} = (\epsilon - (\Delta + k_0^2)^2)u - u^3 - \nu(\nabla u)^2 + \eta(\mathbf{r}, t), \quad (2)$$

where  $u(\mathbf{r}, t)$  is a two-dimensional scalar field,  $\epsilon$  is the distance from pattern onset,  $\nu$  is the strength of a non-variational term [12], and  $\eta$  a random forcing term such that  $\langle \eta(\mathbf{r}, t)\eta(\mathbf{r}', t') \rangle = 2F\delta(\mathbf{r} - \mathbf{r}')\delta(t - t')$ , where  $F$  controls the strength of the noise.

For the formation of textures in (2), the width of the structure factor  $S(t)$  (i.e., the width of the peak in the azimuthal average of  $\langle \tilde{u}(\mathbf{k}, t)\tilde{u}(-\mathbf{k}, t) \rangle$ ), has been shown to decay in two distinct stages [7].  $S(t) \sim t^{-\frac{1}{2}}$  is obeyed until the peak amplitude of the field  $u(\mathbf{x}, t)$  saturates, beyond which time the pattern coarsens and the decay becomes slower. For  $\epsilon = 0.25$  and  $\nu = 0$ , Cross and Meiron [5], Elder et al. [4], and Hou et al. [8] found that in this second region  $S(t)$  decreased as  $t^{-\frac{1}{5}}$  when  $F = 0$ , and as  $t^{-\frac{1}{4}}$  when  $F \neq 0$  [4,8]. Schober et al. [7] found that for  $F = 0$  and  $\nu = 0$ ,  $S(t) \sim t^{-\frac{1}{4}}$ ; the discrepancy with earlier results could be due to the one-dimensionality of their model.

The characterization of pattern formation in model systems using  $\bar{\delta}(\beta)$  has also shown the presence of two stages: the emergence of domains characterized by  $\bar{\delta}(\beta) \sim t^{-\sigma_E(\beta)}$  with  $\sigma_E(\beta) = \frac{1}{2}\beta$ , and a slower coarsening behavior [12]. The relaxation exponent during coarsening depends on the value of  $\nu$  in (2), and is thus expected to be system and model dependent [13]. We report analogous behavior in the present laboratory study of pattern formation in an oscillated granular layer and present additional differences between the two stages.

Our experiments generate patterns in a layer of 0.165 mm bronze spheres contained in a vertically oscillated circular container with diameter 14 cm [14]. The layer is four particle diameters deep, and the cell is evacuated to 4 Pa to avoid any hydrodynamic interaction between the grains and surrounding gas. The control parameters are the frequency  $f$  of the sinusoidal oscillations and the peak acceleration of the container,  $\Gamma = (2\pi f)^2 A^2/g$ , where  $A$  is the maximum amplitude of the oscillation and  $g$  is the gravitational acceleration. As  $f$  and  $\Gamma$  are varied, a variety of

textures including striped, square or hexagonal planforms are observed [14]. Our analysis reported here is restricted to patterns with square planforms. In the region of the phase diagram studied, square patterns appear for increasing control parameter at  $\Gamma \approx 2.75$ ; the bifurcation is subcritical. The geometry of the circular container allows relaxation to an almost perfect square array through wavelength adjustment of the pattern at the container wall over a distance of less than one wavelength [15].

The granular surface is illuminated with a ring of LEDs surrounding the cell. The light is incident at low angles and the scattering intensity is a nonlinear function of the height of the layer; scattering from peaks (valleys) creates bright (dark) regions. The images are collected at the driving frequency and the acceleration of the container is monitored during each run.  $\Gamma$  is suddenly increased from its initial value of 2.2, where no discernible structure is observed. As the grains are not in contact with the container for part of their motion, we assume that the initiation of the quench occurs at the first layer-plate collision after the change of control parameter. The uncertainty in the time origin is the dominant source of error in our measurements.

The top row of Fig. 1 shows that local square domains emerge and coarsen to a final, almost perfect, square array. The bottom row shows this process in Fourier space. A repetition of the experiment would lead to similar, but not identical, intermediate states. Our aim is to study configuration-independent aspects of this relaxation, and to analyze their dependence on the control parameters  $f$  and  $\Gamma$ .

Patterns such as those shown in the top row of Fig. 1 can be represented by a discrete sampling of a smooth scalar field  $v(\mathbf{x})$ . The values of the field are known on a (typically square) grid, but the analytical form of the field is unknown. The ingredients used to deduce the form of the disorder function in (1) are its invariance under arbitrary rigid motions of the texture and the nature of the local planform. Local deviations of a pattern from squares (due to curvature of the contour lines [9]) contribute to  $\bar{\delta}(\beta)$  through the Laplacian, while variations of the size of squares contribute via the choice of a “global”  $k_0$ , which is obtained from the field  $v(\mathbf{x})$  by minimizing the value of  $\bar{\delta}(1)$  [12]. Unlike the information contained in the structure factor,  $|(\Delta + k_0^2)v(\mathbf{x})|$  is a local density of irregularities in the texture, and hence distinct “moments”  $\beta$  can be used to quantify multiple aspects of the disorder density.

The images shown in Fig. 1 have sharp changes at the edges which lead to high frequency contributions in their Fourier spectra. Their removal through simple filtering causes contamination of the pattern near the edges and leads to error in calculating  $\bar{\delta}(\beta)$ . We use a method of noise filtering that involves extending the image to a periodic one using “Distributed Approximating Functionals” (DAFs) [16,17]. Fourier filtering can then be used on the extended image to eliminate high frequency noise and undesirable harmonics [18]. The evaluation of  $\bar{\delta}(\beta)$  requires an accurate estimation of  $\Delta v(\mathbf{x})$ , which typically amplifies any noise present in the discrete, digital experimental data. A method for this calculation has been presented in [9].

The behavior of  $\bar{\delta}(1)$  for the relaxation of Fig. 1 is shown by the symbols  $\circ$  in Fig. 2. The initial formation of local rectangular domains and the final coarsening correspond to distinct power law decays of  $\bar{\delta}(1)$ . The transition coincides with the saturation of the peak amplitude; i.e., nonlinear effects are negligible during domain formation (typically 4-5 oscillations) and become relevant during coarsening [7].

During the initial stage of pattern formation  $\bar{\delta}(1) \sim t^{-0.49 \pm 0.02}$ . This dynamical scaling is similar to that describing the decay of the width of the structure factor [4] and is related to the rate of domain growth in phase ordering kinetics [20,21].

Since nonlinear effects are negligible during domain formation, the evolution can be modeled by (2) with the removal of the nonlinear and stochastic terms. Numerical integration starting from states consisting of random or Gaussian noise shows that  $\int d^2x |u(\mathbf{r}, t)| \sim e^{\epsilon t} t^{-\frac{1}{4}}$  and  $\int d^2x |(\Delta + k_0^2)u(\mathbf{r}, t)| \sim e^{\epsilon t} t^{-\frac{3}{4}}$ ; consequently  $\bar{\delta}(1) \sim t^{-\frac{1}{2}}$ . It has been shown analytically that the width of the structure factor for evolution of  $u(\mathbf{r}, t)$  decays like  $S(t) \sim t^{-\frac{1}{2}}$  until the peak amplitude saturates [7], providing further evidence for the interpretation that the spatiotemporal dynamics is linear during the first stage.

Furthermore, during the domain forming stage, moments of the disorder function decay as  $\bar{\delta}(\beta) \sim t^{-\sigma_E(\beta)}$ , where  $\sigma_E(\beta) \approx \frac{1}{2}\beta$  (see Fig. 3(a)). Analogous behavior can also be seen by numerical integration of the linear terms in (2). The linearity of  $\sigma_E(\beta)$  and the value of the proportionality constant suggest that multiple aspects of textures, such as structure factor, curvature of contours and defect densities decay via a single mechanism during the domain forming stage.

The initiation of domain coarsening coincides with the saturation of peak heights of the granular layer (see Fig. 2); i.e., the latter stages of pattern formation correspond to nonlinear spatiotemporal dynamics of the field [7]. The observed scaling of the disorder function is more complex. For the evolution shown in Fig. 2 at  $\Gamma = 2.8$ ,  $\bar{\delta}(1) \sim t^{-0.18}$  [22]. This is close, but not identical to the rate of relaxation of the structure factor [4,5,7]. Even though the moments  $\bar{\delta}(\beta)$  decay (approximately) as power laws  $t^{-\sigma_L(\beta)}$ , the exponent is not linearly related to  $\beta$  as during the early phase, see Fig. 3(b). There is a tendency towards slower relaxation in Fig. 3(b) (compared to Fig. 3(a)) for larger values

of  $\beta$ . Since large values of  $\beta$  preferentially weight pattern defects, this is consistent with the slower relaxation of the density of defects [8] than that of the structure factor [4,5,7].

The nonlinearity of  $\sigma_L(\beta)$  implies that pattern relaxation occurs on more than one length scale. If the “envelope” of the texture depends on a single length scale  $L(t)$ , the field can be locally expanded as  $u(\mathbf{x}, t) = \text{Re}[e^{i\mathbf{k}\cdot\mathbf{x}} A(\mathbf{X}, t)]$ , where  $\mathbf{X} = \mathbf{x}/L(t)$ ; thus

$$(\Delta + k_0^2)u(\mathbf{x}, t) = \text{Re}\left[e^{i\mathbf{k}\cdot\mathbf{x}}\left(\frac{2i}{L}\mathbf{k}\cdot\nabla_{\mathbf{X}}A - \frac{1}{L^2}\Delta_{\mathbf{X}}A\right)\right].$$

Since  $L(t) \gg k_0^{-1}$  during domain coarsening, the last term can be neglected, leading to

$$|(\Delta + k_0^2)u(\mathbf{x}, t)| \approx \frac{2}{L(t)}\mathbf{k}\cdot\nabla A \sim \frac{|u|}{L(t)}.$$

Consequently  $\bar{\delta}(\beta) \sim 1/L^\beta(t) \sim (\bar{\delta}(1))^\beta$ . Thus the nonlinearity of  $\sigma_L(\beta)$  implies that the relaxation during coarsening occurs on multiple time scales.

Next, we briefly consider changes in the behavior of the disorder function as the experimental system is driven further away from the onset of patterns. The decay of  $\bar{\delta}(\beta)$  during domain formation remains unchanged, but the decay rate in the second region decreases with increasing  $\Gamma$ . Similar behavior has been observed with the addition of  $\nu$  in (2) [12].

We have shown that the formation of texture in a vertically oscillated granular layer occurs in two distinct stages. During the initial stage the spatiotemporal dynamics is essentially linear and the disorder function obeys a universal power law  $\bar{\delta}(\beta) \sim t^{-\sigma_E(\beta)}$ , with  $\sigma_E(\beta) \simeq \frac{1}{2}\beta$ ; this simple behavior is also observed in the linearized Swift-Hohenberg equation. Nonlinearity of spatiotemporal dynamics becomes relevant during domain coarsening and  $\bar{\delta}(\beta) \sim t^{-\sigma_L(\beta)}$  where  $\sigma_L(\beta)$  is a nonlinear function of  $\beta$ . The exponent  $\sigma_L(\beta)$  is model and parameter dependent [12]. Such non-universal, configuration independent characteristics of pattern formation can be used to determine the validity and limitations of model systems [23].

Although dynamical scaling has been reported in the formation of patterns in model systems [4,5,8,12], ours is the first reported observation of stages exhibiting trivial (i.e., a single scaling index such that  $\bar{\delta}(\beta) \sim (\bar{\delta}(1))^\beta$ ) and nontrivial scaling during pattern formation in an experimental system. The methods introduced here are expected to have applications in studying other aspects of textures, such as the quantitative description of patterns in magnetic bubble material [24,25].

We have benefited from discussions with M. Golubitsky, J. B. Swift and P. Umbanhower. The research at the University of Texas was supported by the Engineering Research Program of the Office of Basic Energy Sciences of the U.S. Department of Energy. Additional support came from the Office of Naval Research (GHG), the Ames Laboratory of the Department of Energy (DKH), the National Science Foundation (GHG, DJK), and the R. A. Welch Foundation (DJK).

- 
- [1] R. E. Rosensweig, *Ferrohydrodynamics* (Cambridge University Press, Cambridge, 1985); M. S. Heutmaker and J. P. Gollub, Phys. Rev. A **35** 242 (1987); Q. Ouyang and H. L. Swinney, Nature (London) **352**, 610 (1991).
  - [2] M. C. Cross and P. C. Hohenberg, Rev. Mod. Phys. **65**(3), 851 (1993).
  - [3] E. Wigner, *Symmetries and Reflections* (Greenwood Press, Westport, Connecticut, 1978).
  - [4] K. R. Elder, J. Viñals, and M. Grant, Phys. Rev. A **46**, 7618 (1992).
  - [5] M. C. Cross and D. I. Meiron, Phys. Rev. Lett. **75**, 2152 (1995).
  - [6] J. J. Christensen and A. J. Bray, Phys. Rev. E **58**, 5364 (1998).
  - [7] H. R. Schober, E. Allroth, K. Schroeder, H. Müller-Krumbhaar, Phys. Rev. A **33**, 567 (1986).
  - [8] Q. Hou, S. Sasa, and N. Goldenfeld, Physica A **239**, 219 (1997).
  - [9] G. H. Gunaratne, D. K. Hoffman, and D. J. Kouri, Phys. Rev. E **57**, 5146 (1998).
  - [10] H. G. E. Henschel and I. Procaccia, Physica **8D**, 835 (1983).
  - [11] T. Halsey, M. H. Jensen, L. P. Kadanoff, I. Procaccia, and B. Shraiman, Phys. Rev. A **33**, 1141 (1986).
  - [12] G. H. Gunaratne, A. Ratnaweera, and K. Tennekone, Phys. Rev. E **59**, 5058 (1999).
  - [13] Additional quantities have been measured in the second relaxation region. Hou et al. measured total domain wall length in  $v$  as a function of time. For  $F = 0$ , it was shown to decay as  $t^{-\frac{1}{4}}$ , while for  $F \neq 0$  the decay was proportional to  $t^{-0.3}$ .

Cross et al. showed that a stripe orientation correlation field decayed as  $t^{-0.24}$ . The interpretation of these results is that different measures probe different features of the pattern, and these features evolve via different mechanisms.

- [14] F. Melo, P. Umbanhowar, and H. L. Swinney, Phys. Rev. Lett. **75**, 3838 (1995).
- [15] Experiments done in square containers also exhibit our main results. However, the formation of a single domain takes a much longer time, as the final pattern orientation is strongly constrained by the boundaries.
- [16] D. K. Hoffman, G. H. Gunaratne, D. S. Zhang, and D. J. Kouri, Chaos **10**, 240 (2000).
- [17] D. K. Hoffman, M. Arnold, and D. J. Kouri. J. Phys. Chem. **96**, 6539 (1992); D. K. Hoffman and D. J. Kouri, Proceedings of the Third International Conference on Mathematical and Numerical Aspects of Wave Prop. Phenom., SIAM, 1995, pp. 56-83.
- [18] Calculations reported here are performed by a preliminary estimate of the wave-vector  $k_t$  (the wave-vector of the peak of the radial average of the power spectrum), followed by the filtering of spectral components outside  $[0.7k_t, 1.3k_t]$ . The trends reported here do not depend on the range of spectral components retained.
- [19] W. H. Press, B. P. Flannery, S. A. Teukolsky and W. T. Vetterling, *Numerical Recipes - The Art of Scientific Computing* (Cambridge University Press, Cambridge, 1988).
- [20] A. J. Bray, Adv. Phys. **43**, 357 (1994).
- [21] Our data cannot differentiate between a decay of  $t^{\frac{1}{2}}$  and a possible decay  $(t/\log t)^{-\frac{1}{2}}$  in the presence of defects; see A. J. Bray, A. J. Briant, and D. K. Jarvis, preprint, cond-mat/9902362.
- [22] This index is not expected to be universal; see Ref. [9].
- [23] For e.g., S. C. Venkataramani and E. Ott, Phys. Rev. Lett. **80**, 3495 (1998).
- [24] P. Molho, J. Gouzerh, J. C. S. Levy, and J. L. Porteseil, J. Magn. Magn. Mat. **54-57**, 857 (1986).
- [25] K. L. Babcock and R. M. Westervelt, Phys. Rev. A **40**, 2022 (1989).

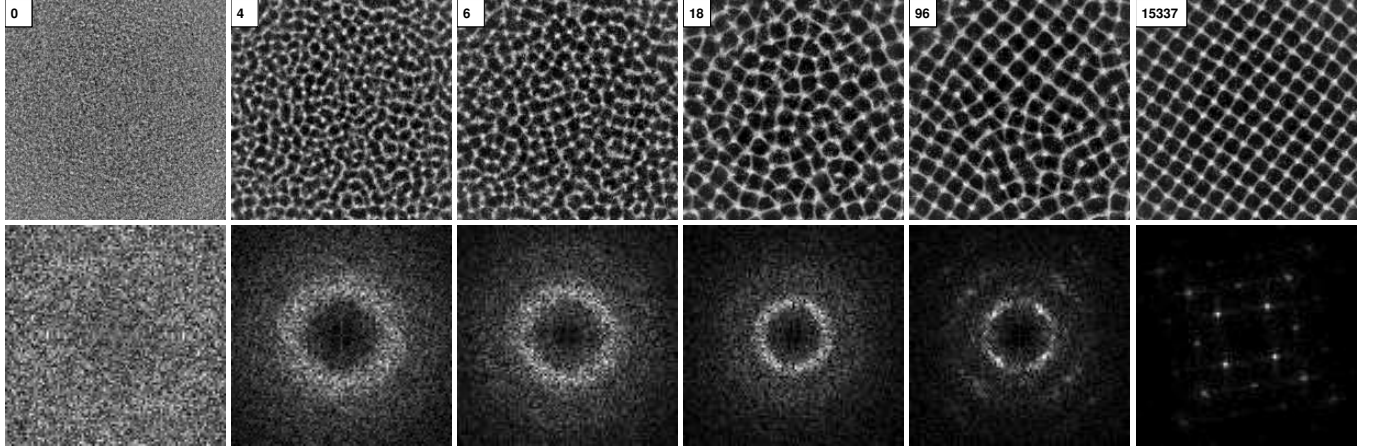


FIG. 1. Snapshots showing the emergence of a square spatial pattern in a granular layer at  $f = 27$  Hz and  $\Gamma = 2.8$ ; the times given in the upper left corner of each image are in units of container oscillation periods. Each image in the first row is of the central 8 cm of the 14 cm diameter circular container. Each image in the second row is the Fourier transform of the image above it. In the first row, the first three frames show the emergence of local domains from a uniform background, and the last three show the slower coarsening of these domains to an almost perfect square array.

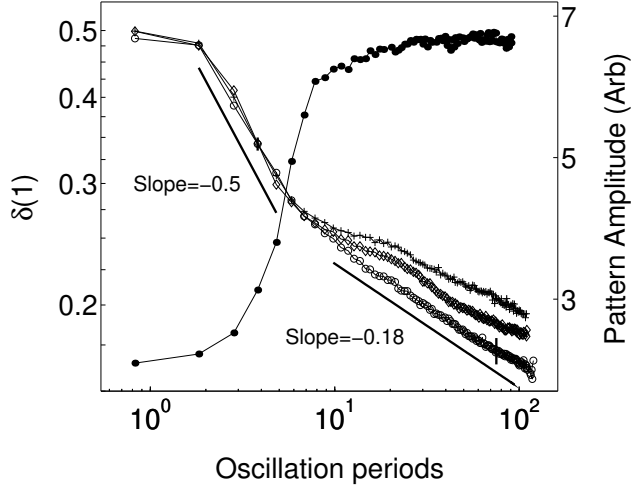


FIG. 2. The time evolution of the disorder function  $\bar{\delta}(1)$  for square patterns at three different final container accelerations,  $\Gamma = 2.8$  ( $\circ$ ),  $\Gamma = 3.0$  ( $\diamond$ ), and  $\Gamma = 3.2$  ( $+$ ). Also shown is growth of the pattern amplitude at  $\Gamma = 2.8$  ( $\bullet$ ). Rapid early growth in the domain-forming phase is followed by a saturation of the amplitude in the coarsening phase. Each curve is an average of 10 runs at the same control parameters. The error bar at late times for  $\circ$  shows typical variation between distinct runs. The error bars at early times are the size of the symbols.

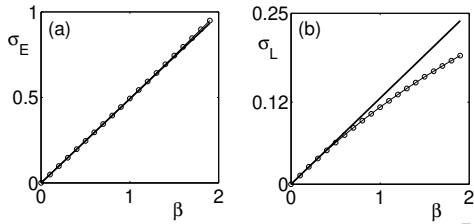


FIG. 3. The slopes  $\sigma_E(\beta)$ ,  $\sigma_L(\beta)$  of the curves  $\bar{\delta}(\beta)$  during (a) domain formation and (b) coarsening. The results are for a single run at control parameters  $f = 27$  Hz and  $\Gamma = 3.0$ . The bold straight lines are drawn to guide the eye. In (a), the bold line has slope  $= 1/2$  and in (b), the bold line has slope  $= 0.12$ .